Rhinology

Thermal water delivery in the nose: experimental results describing droplet deposition through computational fluid dynamics

Distribuzione dell'acqua termale a livello nasale: studio sperimentale della deposizione di microgocce mediante fluidodinamica computazionale

E.F.M. BUIJS[1], V. COVELLO[2], C. PIPOLO[1], A.M. SAIBENE[1], G. FELISATI[1], M. QUADRIO[2]

[1] Unit of Otolaryngology, Department of Head and Neck Surgery, ASST Santi Paolo e Carlo, Department of Health Sciences, Università degli Studi di Milano, Italy; [2] Department of Aerospace Sciences and Technologies, Politecnico di Milano, Italy

SUMMARY

Thermal water therapies have a role in treating various inflammatory disorders dating back to ancient Greece. Several studies have demonstrated beneficial effects of thermal water inhalations for upper respiratory disorders, such as improvement of mucociliary function and reduction of inflammatory cell infiltration. This experimental study describes the numerical investigation and clinical implications of thermal water droplet deposition in the nasal cavity of a single patient. To our knowledge, the numerical flow simulations described are the first investigations specifically designed for thermal water applications. To simulate nasal airflow, a patient-specific 3D computer model was created from a CT scan. The numerical approach is based on the Large Eddy Simulation (LES) technique and builds entirely upon open-source software. Deposition on mucosa was studied for two droplet sizes (5 and 10 μm diameter), corresponding to common thermal therapy applications (aerosol and vapour inhalation). The simulations consider steady inspiration at two different (low and moderate) breathing intensities. The results of this preliminary study show specific deposition patterns that favour droplet deposition in the middle meatus region to the inferior meatus, with particle size- and breathing intensity-related effects. These global data on particle deposition differ from findings related to the single-phase nasal airflow, which is more evenly distributed between the middle and inferior meatus. The potential clinical consequences of deposition data are discussed. The study furthermore provides evidence for the effectiveness of thermal aerosol and vapour inhalation therapies in reaching important areas of nasal mucosa with considerable clinical significance.

KEY WORDS: Thermal water • Aerosol • Vapour Inhalation • Computational Fluid Dynamics • Paranasal sinuses

RIASSUNTO

La terapia inalatoria termale viene utilizzata sin dall'antica Grecia come presidio antiinfiammatorio. Numerosi studi hanno dimostrato una efficacia clinica delle terapie inalatorie termali, quali ad esempio un miglioramento della funzione mucociliare o la riduzione dell'infiltrazione di cellule infiammatorie. Scopo di questo studio sperimentale è realizzare nell'uomo un'analisi numerica e discutere le implicazioni cliniche della deposizione di gocce di acqua termale nella cavità naso-sinusale di un paziente. Le simulazioni numeriche presentate in questo lavoro sono, a conoscenza degli autori, le prime specificamente progettate per lo studio della deposizione di acqua termale. Per la simulazione del flusso nasale, è stato realizzato un modello computerizzato 3D a partire da immagini TC. È quindi stata effettuata una simulazione numerica del flusso mediante Large Eddy Simulation (LES), utilizzando software open-source. Al fine di studiare le più comuni terapie inalatorie termali (aerosol e inalazioni) sono state prese in esame particelle di due dimensioni diverse (5 e 10 μm di diametro). La simulazione del flusso nasale è stata effettuata in condizioni di inspirazione stazionaria in corrispondenza di due diversi livelli di intensità respiratoria (bassa e moderata). I risultati di questo studio preliminare hanno evidenziato dei pattern specifici di deposizione delle particelle che tendono a privilegiare la regione del meato medio rispetto a quella del meato inferiore, con differenze dei risultati al modificarsi dei parametri relativi alle dimensioni delle particelle o dell'intensità di respiro. Il dato globale sulla deposizione non coincide con quello relativo al campo di moto del flusso nasale, che non mostra differenze così significative fra la regione del meato medio e quella del meato inferiore. Vengono discusse le possibili ricadute cliniche di tali dati. I risultati di questo studio dimostrano l'efficacia delle cure termali aerosol e inalazione nel raggiungere le zone della mucosa di maggiore importanza dal punto di vista clinico.

PAROLE CHIAVE: *Acqua Termale • Aerosol • Inalazione • Fluidodinamica Computazionale • Seni Paranasali*

Introduction

Thermal waters, such as sulphurous, oligomineral and radioactive, are widely used to treat various inflammatory disorders of the upper respiratory tract. Their clinical application dates back to ancient Greece. Each type of thermal water, classified on its physical and chemical properties, possesses its own specific therapeutic functions [1 2]. Traditional techniques to treat sinonasal diseases include aerosols, inhalations and nasal douches [1-4]. Various studies have described the beneficial effects of commonly used thermal waters on the respiratory mucosa, such as improvement of mucociliary activity and reduction of inflammatory parameters of nasal cytology [3 4]. Some studies also describe the *in vitro* effects of thermal waters, i.e. their antioxidant and anti-elastase effects [5 6].

Various techniques such as aerosol, inhalation and irrigations have been studied and developed to properly deliver beneficial thermal waters to the complex nasal cavity [1 2]. Nasal irrigations have been shown to effectively wash the sinonasal cavities, overcoming nasal anatomical variations such as septal deviations, especially when performed with high volumes [7]. However, a complete understanding of the process of droplet deposition in thermal water dispersant techniques, such as aerosols and inhalations, is still lacking. Improving our insight could be extremely important for both its scientific and clinical implications, for example in understanding drug delivery, targeted treatment and further development of devices.

In recent years, the *in silico* approach is providing an interesting alternative to *in vivo* and *in vitro* studies. In particular, there have been significant advances in Computational Fluid Dynamics (CFD), which nowadays offers interesting opportunities as it provides an accurate and non-invasive quantitative analysis of flows. In the rhinology field, many studies have shown the potential of computed tomography-based CFD in, for example, pre- and post-operative evaluation of nasal flow and surgical planning [8-12]. Several studies have been presented in the literature to understand the droplet deposition process in the nose by means of CFD, employing different anatomical reconstructions and different simulation techniques. It is important to note that airflow in the nose is a complex transitional flow (i.e. developing in both the laminar and turbulent regimes) which takes place in a very complicated anatomical setting. Therefore, published works often chose to simplify the anatomical model, excluding for example relevant structures such as frontal and maxillary sinuses [11-17]. Additionally, many studies have further simplified nasal flow by assuming it entirely laminar [11 18] or contrarily, have considered it entirely turbulent with the effects of turbulence accounted for via the Reynolds-Averaged Navier-Stokes (RANS) equations and a corresponding turbulence model [12 16 17 19]. Large Eddy Simulation (LES) is a different approach to perform CFD. LES embodies a more physically grounded turbulence modelling and potentially brings greater fidelity to the results, at the cost of a larger computational burden [20]. Even though it is quite popular within the CFD community, few studies to date have employed it to simulate nasal flow.

The present experimental study investigates water droplet deposition in the nasal cavity by means of LES and in a complete and patient-specific model. The procedure is based on an entirely open-source software toolchain, whose main elements are 3D Slicer [21] for 3D reconstruction, OpenFOAM (OpenCFD Limited, ESI Group Company, Bracknell, UK) for numerical simulations and Paraview (Kitware, New York, US) for visualisation of the results. Their use for nasal flow simulations has been described in a previous work from our group [22]. Both inhalation and aerosol therapies are considered in an effort to improve the current understanding of nasal flow and droplet deposition, with a focus on possible clinical implications. We underline that in this paper we study a natural, low-intensity inspiration of ambient air with suspended droplets, and our results are not specifically tied to a specific nebuliser.

Materials and methods

The study was approved by the internal Ethics Committee of San Paolo Hospital, Milan. A CT scan of a 67-year-old Caucasian male was selected from a library of approximately 50 scans belonging to patients with no reported nasal symptoms, no history of head and/or face trauma and without a history of chronic rhinosinusitis or sinonasal tract neoplasms. Except for a mild symmetric hypertrophy of the inferior nasal conchae, sinonasal anatomy was considered normal. A plain head CT was performed with a 64-row multi-detector CT (VCT, General Electric Healthcare, Wisconsin, USA), with the patient receiving a 1.9 mSv effective dose. The CT scan has a 512 × 512 matrix with a 0.49 mm × 0.49 mm spatial resolution in the sagittal-coronal plane and a 0.625 mm gap between consecutive axial slices. The entire study consisted of 350 native images. A HU-value of – 218 was selected in order to acquire an anatomically coherent 3D reconstruction of the air-filled cavities. More details on CT, threshold value choice and 3D reconstruction, obtained via the software 3D Slicer, can be found in a previous publication by our group [22].

Nasal thermal water inhalation therapies consist of inhaling vapour droplets through the nose while the mouth re-

mains closed. In order to let the simulation focus on the nasal region, the oral connection is therefore digitally removed in our model. A 3D model of the air volume within the nasal passageways is then created and intersected with an external spherical volume around the nose, as shown in Figure 1 on the left. This tightly adherent external mask-like volume contains droplets to be inhaled at the start of the simulation and is designed to minimise the computational overhead. The tool SnappyHexMesh, part of the open-source CFD library OpenFOAM, is then used to transform the description of the anatomy into a computational finite-volumes mesh, consisting of approximately 25 million cells.

The mathematical model employed for the nasal flow simulations is briefly explained below.

The governing equations of the flow field are the incompressible Navier-Stokes equations. According to the LES technique, the equations are defined by introducing a filtering operation that decomposes the velocity vector u(x,t) into the sum of $u = \tilde{u} + u'$, where u' stands for the residual (or subgrid scale) component, whereas $\tilde{u}$ stands for the filtered (or resolved) component. The filtered field represents the motion of the large eddies (large vortices) only. The filtering operation is related to the grid resolution and allows obtaining adequate resolution of the resulting filtered field on a relatively coarse grid. The behaviour of the residual (or subgrid-scale) component is properly modelled [20]. The filtered form of the Navier Stokes equation is:

$$\nabla \cdot \tilde{u} = 0$$

$$\frac{\partial \tilde{u}}{\partial t} + (\tilde{u} \cdot \nabla)\tilde{u} - v\nabla^2\tilde{u} + \nabla \cdot \tau_{sgs} + \frac{\nabla \tilde{p}}{\rho} = 0$$

In this equation, $\tilde{u}$ denotes the filtered velocity vector, $\tilde{p}$ the filtered pressure, ρ the density and v the kinematic viscosity. The subgrid stress tensor, τ_{sgs} is modelled by the Smagorinsky model [23]:

$$\tau_{sgs} = -2\, v_{sgs}\, \tilde{D}$$

in which v_{sgs} is a scalar function named subgrid eddy viscosity and $\tilde{D}$ is the strain tensor of the filtered velocity field. For further details about the LES technique, see the book by Pope [20].

The motion of the water droplets is mathematically solved by a Lagrangian approach, in which fluid particles are individually followed as they move in time and space, convected by the unsteady flow field. For each droplet, velocity and position are computed as a function of time; droplets are considered as rigid spheres with assigned physical properties, with heat transfer neglected.

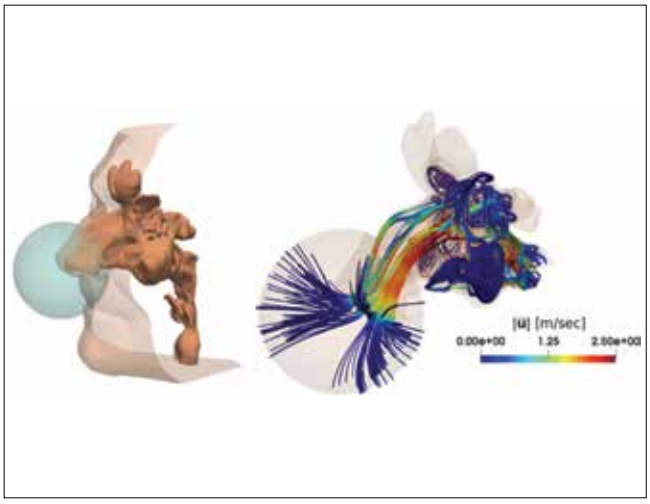

Fig. 1. Left: 3D reconstructed model for flow simulation, including the external volume sphere; **right:** streamlines of the mean flow field, colour-coded for the magnitude of the mean velocity vector.

The LES considered in this work computes the inhalation of air, transporting water droplets, for a time interval of 0.6 seconds. The flow is produced by an imposed pressure difference between the external ambient and the throat; two values for the pressure difference are considered, namely $\Delta p = 10$ Pa and $\Delta p = 20$ Pa. These values correspond to flow rates near to 13 L/min and 20 L/min respectively, which are considered typical of low-and medium intensity breathing [24].

At the initial time, approximately 10^5 quiescent droplets are placed into the spherical volume. For each treatment, the number of droplets per unit volume is extrapolated from literature data [25-27]. As soon as a droplet reaches the mucosal wall, its velocity is set to zero and the particle is considered to be stuck on the wall. Four different simulations were taken from our previous work (Table I) [28]. For this study, a quite detailed mesh size was used, containing approximately 25 x 10^6 cells. Two different droplet sizes are considered of 5 μm and 10 μm, approximating average droplet diameters for aerosol and inhalation treatment respectively [1 2 29].

Results

Flow

We start by providing a qualitative and quantitative assessment of the flow field in the nasal cavity at a pressure difference of 20 Pa. In Figure 1 (right), the streamlines of

Table I. Numerical simulations carried out on a computational mesh of 25 million cells.

Simulation ID	Δ p (Pa)	Particle diameter (μm)
1	10	5
2	10	10
3	20	5
4	20	10

the time-averaged velocity field are shown, colour-coded with the magnitude of the mean velocity vector. The figure emphasises the considerably large velocity values occurring in the meatuses, where the velocity magnitude reaches about 2.5 m/sec, and low, approaching zero but not exactly zero, velocity levels in the paranasal sinuses.

Droplet deposition

In this section we present both qualitative and quantitative assessment for droplet deposition. The quantitative analysis has been validated by comparison of published data (both *in vivo* and *in vitro*) in our previous work [28].

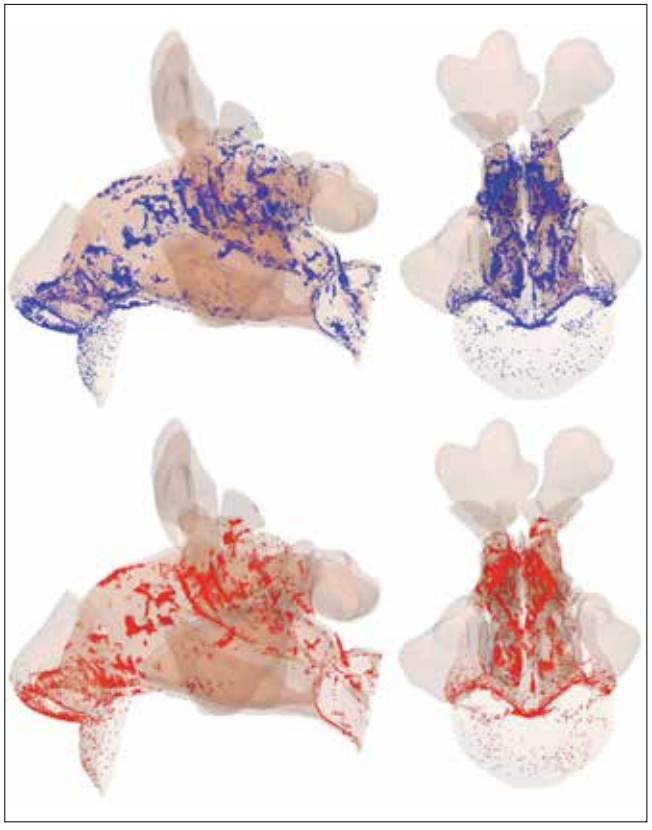

Fig. 2. Top: mucosal droplet deposition of 5 μm particles (blue) at 20 Pa pressure difference; **bottom:** mucosal droplet deposition of 10 μm diameter particles (red) at 20 Pa pressure difference. The lateral view is shown on the left hand side, the frontal view on the right.

A qualitative representation of droplet deposition for Δ p = 20 Pa is shown in Figure 2 in both lateral (left) and frontal views (right). Droplets that, at the end of the simulation time, were still in flight or have exited the computational domain through the laryngeal outflow are not plotted. In the top of the Figure, droplets of 5 μm diameter deposited on the mucosal lining of the nose at the end of the simulation are shown as blue dots. At the bottom of the Figure, the deposition of droplets with the larger, 10 μm, diameter is illustrated in red. Figure 2 refers to simulations labelled as 3 and 4 in Table I.

Figure 2 highlights that deposition takes place over the entire nasal mucosa. In a qualitative evaluation, an evident difference in deposition pattern between the two particle sizes cannot be easily appreciated. In order to describe the mucosal deposition of the droplets in more detail, a quantitative analysis should therefore be performed. For an extensive droplet deposition analysis, the entire surface of the nasal model was divided in 27 slabs, each of approximately 5 mm thickness, along the main axis of the nasal passageways (Fig. 3, left).

Next, the surface density of deposited droplets on each slab was computed. The density D_x on slab x is defined as follows:

$$D_x = \frac{N_x}{A_x}$$

where N_x is the number of particles deposited on slab x, and A_x is the slab area surface in mm^2. Deposition was calculated for both particle sizes, each at a different pressure levels, as seen in the graph of Figure 3 top (Δ p = 10 Pa) and bottom (Δ p = 20 Pa).

In the quantitative analysis of the deposition, interesting differences between particle size and varying pressure levels are observed. Important anatomical landmarks such as the nostrils (slabs 1 and 2), the nasal valve (slabs 3 and 4) and the osteomeatal complex (slabs 14 to 18) can now be more easily identified and studied. At first look, the nostrils show an overall low deposition for both particle sizes at both breathing intensities. In these conditions, the nasal valve area shows a modest peak of deposition, whereas the region of the osteomeatal complex shows an important peak. When we look more in depth by comparing various sizes and intensities, we can observe more details. Particles of 10 μm at low breathing intensity (Fig. 3 top, red line) are observed to deposit mainly on slabs 14-17, corresponding to the anterior part of the middle turbinate. Smaller particles of 5 μm, shown in blue, at this breathing intensity are observed to spread

out more evenly on the entire nasal mucosa and do not produce a clear peak in deposition. When the breathing intensity increases (Figure 3, bottom graph), smaller particles are observed to deposit mainly in the anterior part, presenting peaks at slabs 2 and 3 but also 14 and 16. When comparing the larger particles (in red) at the two pressure differences, an increased peak at slab 25 emerged, corresponding to the posterior part of the middle turbinate and posterior spheno-ethmoidal recess. At slabs 14-17, the deposition of larger particles is 2-5 times larger than that of smaller particles at both breathing intensities. Overall, for both particle sizes, it appears that increasing the pressure difference leads to increased deposition peaks on specific sections. At lower pressure differences, instead, an overall homogeneously distribution over the surface is seen.

In Figure 4, we proposed a further post-processing analysis that focused on a specific area of interest, namely slabs 12 to 17. In this figure, on the left, an arbitrary boundary between the middle and inferior meatus was drawn, as shown by the change in colour. D_p corresponds to the pressure levels. For this particular analysis, both the frontal sinus and maxillary sinus were removed from the anatomy.

Quantitative deposition results for the middle and superior meatus are plotted in Figure 4, top right. Inferior meatus deposition in the ethmoid region is shown in Figure 4, bottom right, where it is key to notice that the scale of D_x is significantly smaller. Especially for slab 14, an important difference can be observed between the top and bottom graphs. In the upper half of slab 14, a peak in droplet deposition is observed at both pressure levels and for both droplet sizes. The lower half of this slab however, remains relatively 'empty'. This difference is especially striking with reference to the red curves, corresponding to larger droplets.

Discussion

Thermal water dispersant therapies are used nowadays not only for upper respiratory problems, but also in lower respiratory diseases such as asthma [1 2]. The most common indications for these thermal water therapies range from chronic sinusitis to chronic nasal polyposis. Given the lack of specific data, there is some debate on the rate of water droplets that once inhaled do not reach the targeted mucosa and may disappear further down the respiratory tract. Both qualitatively and quantitatively, the preliminary results of our study show that important droplet deposition takes place in the ethmoidal region, a site with relevant clinical implications in chronic rhinosinusitis with or without nasal polyps. Peaks of deposition in this region are seen for both particle sizes. It is important to note that the mass of an aerosol particle (5 µm diameter) is 8 times smaller than the mass of an inhalation particle (10 µm diameter). Taking this into account, deposition appears to be even more effective for the larger 10 µm droplets. The results of this experimental study, even though limited to the anatomy of a single patient, is supporting evidence

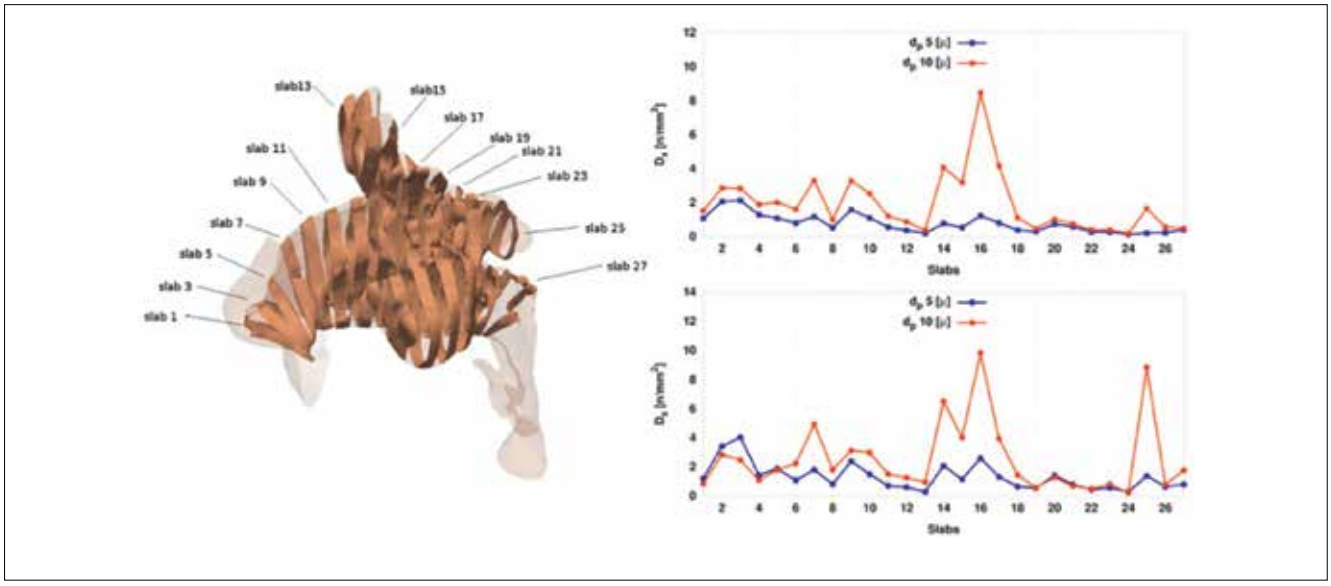

Fig. 3. Left: division of the computational domain into 27 slabs. Only the odd slabs are shown for clarity purposes; **right:** density of droplets (D_x) deposited on slab x for the two particle diameters (d_p) at the pressure levels Δ p = 10 Pa (top graph) and Δ p = 20 Pa (bottom graph).

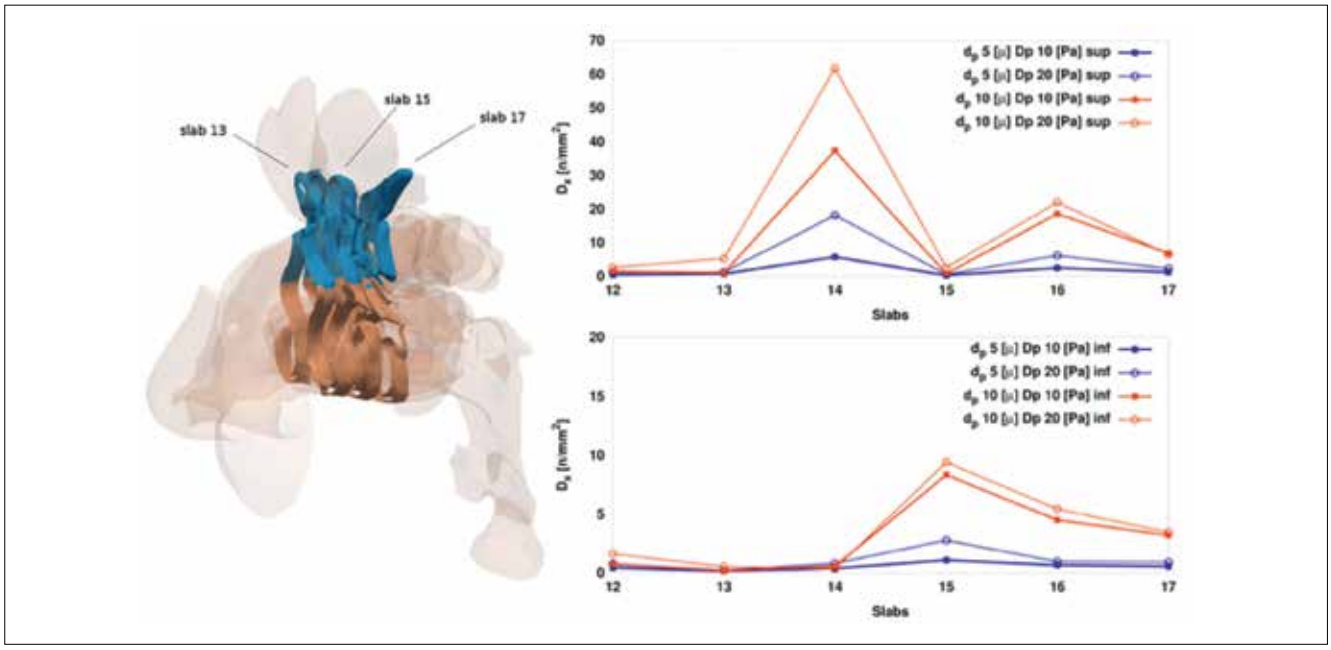

Fig. 4. Left: graphical representation of slabs 12 to 17 dividing the nasal meatuses and excluding frontal and maxillary sinuses. For clarity, only slabs 13, 15 and 17 are drawn in the image; **right:** density for droplets (D_x) deposited on the superior part (top graph) and inferior part (bottom graph), for both pressure levels (D_p) and particle sizes (d_p) analysed.

that current thermal therapies are effective in reaching important areas of nasal mucosa with considerable clinical significance.

To the authors' knowledge, this study is first to investigate, through extensive numerical analysis, droplet deposition in the context of thermal water therapy for the upper respiratory tract and its clinical implications. Nasal flow simulation studies have generally involved RANS simulations and/or simplified anatomical models, as reported in these recent examples of RANS and LES works in simplified nose models [12-16]. However, both approaches may affect the reliability of outcomes for the clinical setting, for example when important anatomical structures such as the maxillary and frontal sinuses are excluded. In the CFD field, LES allows capturing more detail of the complex nasal flow field than the traditional RANS [20]. Even though the detailed reliability of the present results remains to be quantitatively assessed, the extra computational effort required by the LES approach, as well as the consideration of a realistic and complete anatomy, are important to improve the current understanding of nasal flow with CFD.

The LES approach and realistic reconstructed anatomies have brought to light some specific findings that should be taken into account when considering the clinical implication of thermal water treatments. The deposition pattern of therapeutic water particles that stick to the mucosa shows a striking difference between the middle meatus, where significant deposition is observed, and the relatively 'empty' inferior meatus (Fig. 2). The deposition pattern is very interesting since it mimics the distribution pattern of common inflammatory diseases of the nose. Both inflammatory and malignant pathologies are indeed more frequent in the ethmoidal region. On the basis of our results as well as the anatomical analogy with inflammatory diseases, it can be surmised that the deposition of potentially inflammatory/carcinogenic particles might follow a similar distribution, even though these particles have different physical properties that should be further investigated. This CFD-based inference could integrate and support other developmental hypotheses for oncogenesis such as the evo-devo hypothesis [30]. On this basis, our 3D results could be relevant for future studies with large datasets devoted to understanding pathologies of the nose.

The deposition pattern between the ethmoidal region and the inferior meatus is further shown by the quantitative analysis in Figure 4. In this case, an arbitrary boundary between the superior and inferior regions of the nasal cavity was drawn. We can observe a striking difference in overall droplet deposition as well as different peaks. As for the upper part of the nose, the peak of deposition was found to be located more anteriorly, while for the inferior part, the peak of deposition lies more posterior. We must keep in mind, however, that the simulation was done using the normal sinonasal anatomy of a single patient. The effects on droplet deposition patterns through extensive numerical analysis in multiple patients and occurring anatomi-

cal variations (such as septal deviations) is an interesting point for future research and statistical assessments.
In contrary to most of the CFD studies on this topic, we have also attempted to evaluate the droplets that enter the paranasal sinuses, which is important in quantitatively defining the effectiveness of targeted inhalation therapy for inflammatory disorders such as chronic sinusitis. Though computationally quite simple, this evaluation should be considered with care given some methodological limitations. The detailed correct reconstruction of the anatomy of such small structures as the sinus ostia is impeded by the resolution of typical CT scans (which is about the size of the ostium) and by the uncertainty implied by the choice of the HU-threshold for the reconstruction. This is even more crucial in chronic sinusitis patients, where ostia can be reduced or closed off by oedema and/or polyps. Larger and more detailed studies are therefore required to accurately quantify the droplet deposition inside the sinuses. However, our current study shows widespread deposition on the mucosa, including the area around the ostia, suggesting a potential beneficial effect of thermal waters in improving drainage of the sinus.

Conclusions

Deposition of thermal water droplets on the upper respiratory mucosa has been assessed, both qualitatively and quantitatively, through LES numerical simulations in an anatomically accurate domain. A 3D view of the droplet deposition pattern in the human nasal cavity has been obtained; a quantitative and in-depth evaluation of the spatial distribution of deposited droplets has been achieved through the discretisation of the model in 27 slabs of the nasal mucosa. Additional evaluation allowed analysis of deposition in the middle and inferior meatus regions.
This single patient study shows interesting differences in the mucosal deposition pattern for various droplet sizes, corresponding to two well-known thermal treatments. Smaller droplets (5 μm diameter, corresponding to aerosol) are seen to deposit quite evenly in the nasal cavity, where larger droplets (10 μm diameter, corresponding to vapour inhalation) show a deposition in peaks, corresponding to the ethmoid and middle turbinate area. Both qualitatively and quantitatively, our study shows for both therapies a significant droplet deposition in the ethmoidal region, a location of importance in the pathogenesis of polyposis. The results of this experimental groundwork could provide further evidence for the effectiveness of thermal therapies in reaching important areas of nasal mucosa with considerable clinical significance.

Acknowledgements

The present research has been funded by FoRST (Foundation for the Thermal Scientific Research) in the framework of the ATHEWADE project (Assessment of Thermal Water Delivery via computational fluid dynamics). This work has also been made possible by the grant funded by the Serpero Foundation and received for the project "Comparison and validation of innovative methods for nasal fluid dynamics assessment". The authors gratefully acknowledge the computing time obtained by the CINECA Supercomputing Center with the IscraC Onose-Pa Project.

References

1 Agostini G. *Manuale di Medicina Termale*. Second Edition. Torino: Archimedica; 2000.

2 Nappi G, De Luca S, Masciocchi MM. *Medicina e clinica termale*. Pavia: Selecta Medica; 2001.

3 Passali D, De Corso E, Platzgummer S, et al. *SPA therapy of upper respiratory tract inflammations.* Eur Arch Otorhinolaryngol 2013;270:565-70.

4 Staffieri A, Abramo A. *Sulphurous-arsenical-ferruginous (thermal) water inhalations reduce nasal respiratory clearance and improve mucociliary clearance in patients with sinonasal disease: preliminary outcomes.* Acta Otolaryngol 2007;127:613-7.

5 Braga P, Sambataro G, Dal Sasso M, et al. *Antioxidant effect of sulphurous thermal water on human neutrophil bursts: chemiluminescence evaluation.* Respiration 2008;75:193-201.

6 Braga P, Dal Sasso M, Culici M, et al. *Effects of sulphurous water on human neutrophil elastase release.* Ther Adv Respir Dis 2010;4:333-40.

7 Thomas WW, Harvey RJ, Rudmik L, et al. *Distribution of topical agents to the paranasal sinuses: an evidence-based review with recommendations.* Int Forum Allergy Rhinol 2013;3:691-703.

8 Quadrio M, Pipolo C, Corti S, et al. *Review of computational fluid dynamics in the assessment of nasal air flow and analysis of its limitations.* Eur Arch Otorhinolaryngol 2014;271:2349-54.

9 Wang D, Lee H, Gordon R. *Impacts of fluid dynamics simulation in study of nasal airflow physiology and pathophysiology in realistic human three-dimensional nose models.* Clin Exp Otorhinolaryngol 2012;5:181-7.

10 Rhee J, Pawar S, Garcia G, et al. *Toward personalized nasal surgery using computational fluid dynamics.* Arch Facial Plast Surg 2011;13:305-10.

11 Hariri B, Rhee J, Garcia G. *Identifying patients who may benefit from inferior turbinate reduction using computer simulations.* Laryngoscope 2015;125:2635-41.

12 Nomura T, Ushio M, Kondo K, et al. *Effects of nasal septum perforation repair surgery on three-dimensional airflow: an*

evaluation using computational fluid dynamics. Eur Arch Otorhinolaryngol 2015;272:3327-33.

13 Liu Y, Matida EA, Gu J, et al. *Numerical simulation of aerosol deposition in a 3-D human nasal cavity using RANS, RANS/EIM, and LES.* J Aerosol Sci 2007;38:683-700.

14 Liu Y, Matida EA, Johnson MR. *Experimental measurements and computational modeling of aerosol deposition in the Carleton-Civic standardized human nasal cavity.* J Aerosol Sci 2010;41:569-86.

15 Xi J, Kim J, Si X. *Effects of nostril orientation on airflow dynamics, heat exchange, and particle depositions in human noses.* Eur J Mech B Fluids 2016;55:215-28.

16 Chen X, Lee H, Chong V, et al. *Assessment of septal deviation effects on nasal air flow: a computational fluid dynamics model.* Laryngoscope 2009;119:1730-6.

17 Xi J, Si X, Kim J, et al. *Simulation of airflow and aerosol deposition in the nasal cavity of a 5-year-old child.* J Aerosol Sci 2011;42:156-73.

18 Shanley K, Zamankhan P, Ahmadi G, et al. *Numerical simulations investigating the regional and overall deposition efficiency of the human nasal cavity.* Inhal Toxicol 2008;20:1093-100.

19 Si X, Xi J, and Kim J. *Effect of laryngopharyngeal anatomy on expiratory airflow and submicrometer particle deposition in human extrathoracic airways.* O J Fluid Dyn 2013;3:286-301.

20 Pope SB. *Turbulent flows.* IOP Publishing; 2001.

21 Fedorov A, Beichel R, Kalpathy-Cramer J, et al. *3D slicer as an image computing platform for the quantitative imaging network.* Magn Reson Imaging 2012;30:1323-41.

22 Quadrio M, Pipolo C, Corti S, et al. *Effects of CT resolution and radiodensity threshold on the CFD evaluation of nasal flow.* Med Biol Eng Comput 2016;54:411-9.

23 Smagorinsky J. *General circulation experiments with the primitive equations: I. The basic experiment.* Mon Weather Rev 1963;91:99-164.

24 Hooper R. *Forced inspiratory nasal flow-volume curves: a simple test of nasal airflow.* Mayo Clin Proc 2001;76:990-4.

25 Reisner C, Katial RK, Bartelson BB, et al. *Characterization of aerosol output from various nebulizer/compressor combinations.* Ann Allergy Asthma Immunol 2001;86:566-74.

26 Mitchell J, Nagel M. *Particle size analysis of aerosols from medicinal inhalers.* KONA 2004;22:3-65.

27 Djupesland P. *Nasal drug delivery devices: characteristics and performance in a clinical perspective - a review.* Drug Deliv Transl Res 2013;3:42-62.

28 Covello V, Pipolo C, Saibene A, et al. *Numerical simulation of thermal water delivery in the human nasal cavity.* Comput Biol Med 2018;100:62-73.

29 Canzi P. *Tecniche e apparecchiature*. In: *Medicina Termale ORL, Atti del Congresso Nazionale dell'Associazione Italiana Otorinolaringoiatri Liberi Professionisti.* 1984. pp. 9-16.

30 Jankowski R, Márquez S. *Embryology of the nose: the evo-devo concept.* World J Otorhinolaryngol 2016;6:33-40.

Received: June 28, 2018 - Accepted: November 27, 2018

How to cite this article: Buijs EFM, Covello V, Pipolo C, et al. *FThermal water delivery in the nose: experimental results describing droplet deposition through computational fluid dynamics.* Acta Otorhinolaryngol Ital Epub 2019 Jan 31. https://doi.org/10.14639/0392-100X-2250

Address for correspondence: Elvira F.M. Buijs, Università degli Studi di Milano, Unit of Otolaryngology, Department of Head and Neck Surgery, ASST Santi Paolo e Carlo, via Antonio di Rudini 8, 20142 Milan, Italy. Tel. +39 02 8184 4249. Fax +39 02 5032 3166. E-mail: efmbuijs@gmail.com